Nuclear Engineering and Design 313 (2017) 1–9

Contents lists available at ScienceDirect

Nuclear Engineering and Design

journal homepage: www.elsevier.com/locate/nucengdes

Detailed neutronic study of the power evolution for the European Sodium Fast Reactor during a positive insertion of reactivity

A. Facchini [a], V. Giusti [a], R. Ciolini [a], K. Tuček [b], D. Thomas [b], E. D'Agata [b,*]

[a] Department of Civil and Industrial Engineering (DICI), University of Pisa, Largo Lucio Lazzarino 2, I-56126 Pisa, Italy
[b] Joint Research Centre, Institute for Energy and Transport (JRC - IET), European Commission, P.O. Box 2, NL-1755 ZG Petten, The Netherlands

HIGHLIGHTS

- This paper studies the effect of an unexpected runway of a control rod in the ESFR.
- The power peaked fuel pin within the core was identified.
- The increase of the fission power density of the fuel pin has been evaluated.
- Radial/axial fission power density of the power peaked fuel pin has been evaluated.

ARTICLE INFO

Article history:
Received 7 July 2016
Received in revised form 17 November 2016
Accepted 19 November 2016

Keywords:
Sodium Fast Reactor
Neutronic analysis
Unprotected transient of overpower
MCNP calculations
Reactivity accident analysis

ABSTRACT

The new reactor concepts proposed in the Generation IV International Forum require the development and validation of new components and new materials. Inside the Collaborative Project on the European Sodium Fast Reactor, several accidental scenario have been studied. Nevertheless, none of them coped with mechanical safety assessment of the fuel cladding under accidental conditions. Among the accidental conditions considered, there is the unprotected transient of overpower (UTOP), due to the insertion, at the end of the first fuel cycle, of a positive reactivity into the reactor core as a consequence of the unexpected runaway of one control rod. The goal of the study was the search for a detailed distribution of the fission power, in the radial and axial directions, within the power peaked fuel pin under the above accidental conditions. Results show that after the control rod ejection an increase from 658 W/cm^3 to 894 W/cm^3, i.e. of some 36%, is expected for the power peaked fuel pin. This information will represent the base to investigate, in a future work, the fuel cladding safety margin.

1. Introduction

The Generation IV International Forum (GIF) Roadmap (Kelly, 2014) identifies fast reactors as an exceptional, potentially sustainable energy source, particularly in terms of waste management and nuclear fuel optimization. Nearly 55 years of technological experience gained from related projects in many countries have placed the Sodium-cooled Fast Reactor (SFR) in a unique position among the different systems promoted by the GIF. Many countries demonstrated significant advancements on SFRs technology not only in terms of design but also in terms of operation. The Experimental Breeder Reactor (EBR) and the Fast Flux Test Facility (FFTF) in USA, the BN series reactors in Russia and the prototype Phénix and commercial SuperPhénix in France have added over 400 reactor-years of operational experience in the SFR technology. Latest examples of SFRs are the recently connected to the grid China Experimental Fast Reactor (CEFR) (Mi, 1999), the Russian BN-800 (Saraev et al., 2010) and the Indian Prototype Fast Breeder Reactor (PFBR) (Chetal et al., 2006). Also in Europe there are research activities on the SFR field. The European Sustainable Nuclear Industrial Initiative (ESNII), under the umbrella of Sustainable Nuclear Energy Technology Platform (SNETP), has planned an industrial project for demonstration purposes called Advanced Sodium Technological Reactor for Industrial Demonstration (ASTRID). The present work is part of the Collaborative Project on the European Sodium Fast Reactor (CP-ESFR), which has been initiated as part of the EURATOM FP7 contribution to the GIF and an attempt to create a common European framework to support the SFR technology, establishing the technical basis of a European Sodium Fast Reactor with improved safety performance, resource efficiency and cost efficacy (Fiorini and Vasile, 2011). In particular, the study here presented is focused on the determination of the fission power distribution within the power peaked fuel pin at the

* Corresponding author.
E-mail address: elio.dagata@ec.europa.eu (E. D'Agata).

http://dx.doi.org/10.1016/j.nucengdes.2016.11.014
0029-5493/

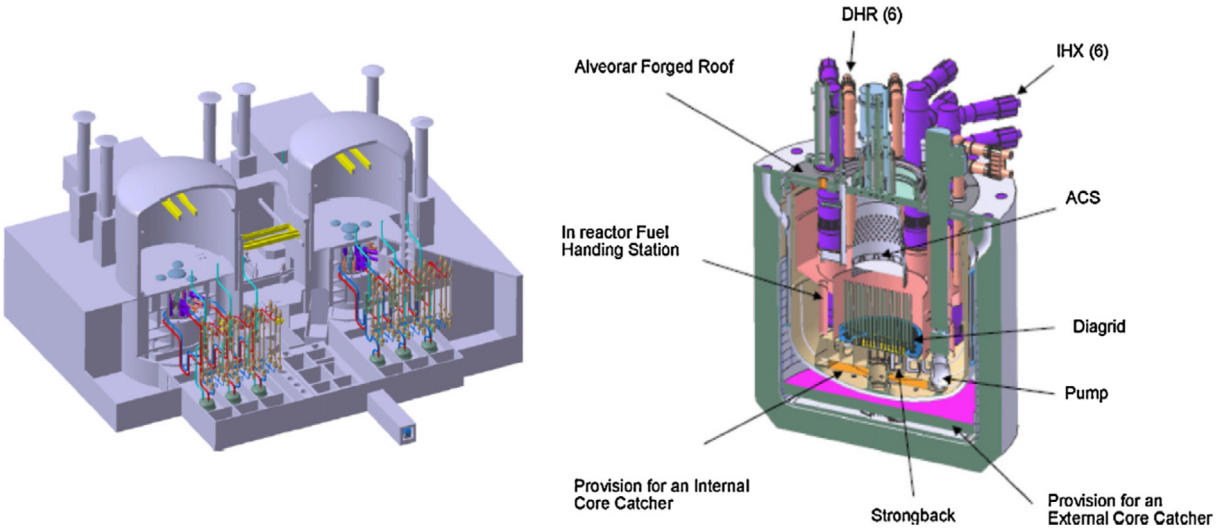

Fig. 1. ESFR plant design and pool type concept for the reactor core (Lazaro et al., 2014).

end of the first fuel cycle (EoC) under accidental conditions. The accidental scenario taken into consideration is the unprotected transient of overpower (UTOP) due to an unexpected runaway of one control rod (a scenario which is also part of the classical design basis accidents). The results of this analysis, part of the preliminary safety analysis of the reactor core, will drive a future work to investigate the pellet-cladding mechanical interaction (PCMI).

The Monte Carlo code MCNP6 (Goorley et al., 2012) has been used for all the calculations here presented. This code differs from its predecessors being the first which integrates all the features of MCNP5 and MCNPX providing, among the others, the capability to perform burnup calculations with the depletion code CINDER90 (Wilson et al., 1995). However, being MCNP6 a steady-state code, the analysis of the UTOP accident will be limited to the instant at which the control rod is ejected from the core. On the other hands, no transient kinetics codes would allow to describe the geometry and perform the neutron transport with the same degree of accuracy achievable with MCNP6. Moreover, the results will be conservative as the neutronic feedback due to the Doppler effect will not be present, not being considered the increase of the fuel temperature during the transient.

2. Core, specifications and MCNP6 model of the European Sodium Fast Reactor

2.1. Core description and specifications

A detailed description of the plant design of the European Sodium Fast Reactor (ESFR) can be found in Fig. 1, designed in Ammirabile and Tsige-Tamirat (2013). The present core design makes use of a fuel based on mixed oxides of uranium and plutonium and it refers to a reactor power of 3600 MW_{th}. The main parameters of the reactor core are reported in Table 1. This section aims at providing the major characteristics of this core design useful for the neutronic modeling purposes.

Fig. 2 represents a horizontal cross section of the core, showing different zones: the inner and outer fuel assembly zones (purple and light blue[1], respectively) and the reflector assembly zone (yellow, to be noted that there is also a reflector assembly in the center of the reactor core). The inner and outer fuel zones are, respectively, made by 225 and 228 assemblies, each one containing 271 fuel pins, and, in order to flatten the core power distribution at the EoC, are characterized by different plutonium mass content (12.80% and 14.90%, respectively) and uranium mass content (75.28% and 73.18%, respectively). The assumed fresh fuel composition for both the inner and outer zone is reported in Table 2. It can be noted that to take into account the beta decay of ^{241}Pu a small fraction of ^{241}Am is also present in the fresh fuel composition.

The fuel assembly consists of a hexagonal wrapper tube, made of a chromium ferritic/martensitic steel (EM10, 9Cr-1Mo), that contains a triangular arrangement of fuel pins with a helical wire wrap spacers to minimize their displacement. The MOX fuel pin is made by pellets with an oxide dispersion strengthened (ODS) steel cladding. Finally, the main characteristics of the fuel assembly are summarized in Table 3.

Fig. 2 shows also the 24 control shutdown devices (CSD) and the 9 diverse shutdown devices (DSD). The CSD rods contain natural boron carbide (~20% of ^{10}B) whereas the DSD rods are made of enriched boron carbide (~90% of ^{10}B). Both the CSD and the DSD rods have a follower which is made of steel and sodium (8% and 92% by weight, respectively). The CSD rods are located, according to a symmetric pattern within the two fuel zones, on two different rings while a single ring of DSD rods is placed between them. The CSD rods are expected to be used during the normal operation to control the long term reactivity changes, the DSD rods are instead

Table 1
ESFR pool-type concept core design specifications (Ammirabile and Tsige-Tamirat, 2013).

ESFR core parameters	
Thermal power	3600 MW_{th}
Volume	17.5 m^3
Lattice pitch	21.08 cm
Fuel type	Pins/Pellets
Active height	1 m
Cladding material	ODS steel
Pin diameter	9.43 mm
Pin per assembly	271
Fuel assemblies	453
Control shutdown devices (CSD)	24
Diverse shutdown devices (DSD)	9
Fraction of delayed neutrons	390 pcm
Core inlet temperature	395 °C
Core outlet temperature	545 °C
Fuel pellet material	(U, Pu)O_2

[1] For interpretation of color in Fig. 2, the reader is referred to the web version of this article.

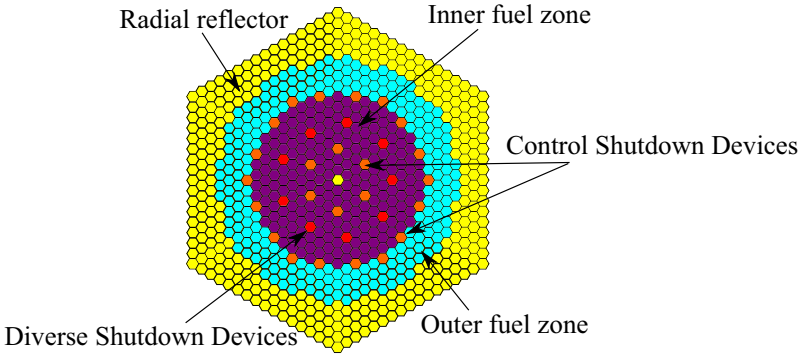

Fig. 2. Horizontal view for the MOX core with different internals.

Table 2
Isotopic mass fraction of the fuel in the two different zones of the ESFR core at BoL.

Isotopes	Inner fuel zone (%)	Outer fuel zone (%)
^{235}U	0.19	0.18
^{238}U	75.09	73.00
^{238}Pu	0.46	0.54
^{239}Pu	6.12	7.11
^{240}Pu	3.83	4.45
^{241}Pu	1.06	1.24
^{242}Pu	1.34	1.56
^{241}Am	0.10	0.17
^{16}O	11.81	11.75

Table 3
Fuel assembly main characteristics.

Design characteristics	
Sodium gap width inter assembly	0.45 cm
Wrapper tube outer flat-flat width	20.63 cm
Wrapper tube thickness	0.45 cm
Wrapper tube material	EM10
Wire wrap spacer diameter	0.1 cm
Wire wrap helical pitch	22.5 cm
Wire wrap spacer material	EM10
Outer clad diameter	10.73 mm
Inner clad diameter	9.73 mm

activated only in case of an emergency shutdown of the reactor (SCRAM). The radial reflector (see again Fig. 2) is axially homogeneous, consists of 3 rings of assemblies and, presently, it is considered as made of a mixture of sodium, low carbon steel (F17) and EM10 (Fiorini and Vasile, 2011). The axial composition of the different reactor core elements is sketched in Fig. 3. The active height of the fuel zones is one meter. The core is axially reflected by a bottom and top reflector with a thickness of 30 and 70 cm, respectively. A fission gas plenum is located both at the top of the fuel (11 cm high) and below the bottom reflector (91 cm high).

The targeted fuel residence time is equal to, at least, 2050 equivalent full power days (EFPD). The average and maximum core burnup are respectively 100 GWd/t and 145 GWd/t for an average power density of 206 W/cm^3 (Fiorini and Vasile, 2011).

2.2. The MCNP6 model

A computational core model for the Monte Carlo code MCNP6 was developed at the Joint Research Centre - Institute for Energy and Transport (JRC - IET) (Fiorini and Vasile, 2011). However, some modifications of this model were in order. According to the aim of the present study, to find the fuel pin compositions at the end of the first fuel cycle it is necessary to perform a burnup calculation over the whole fuel cycle length starting from the fresh fuel com-

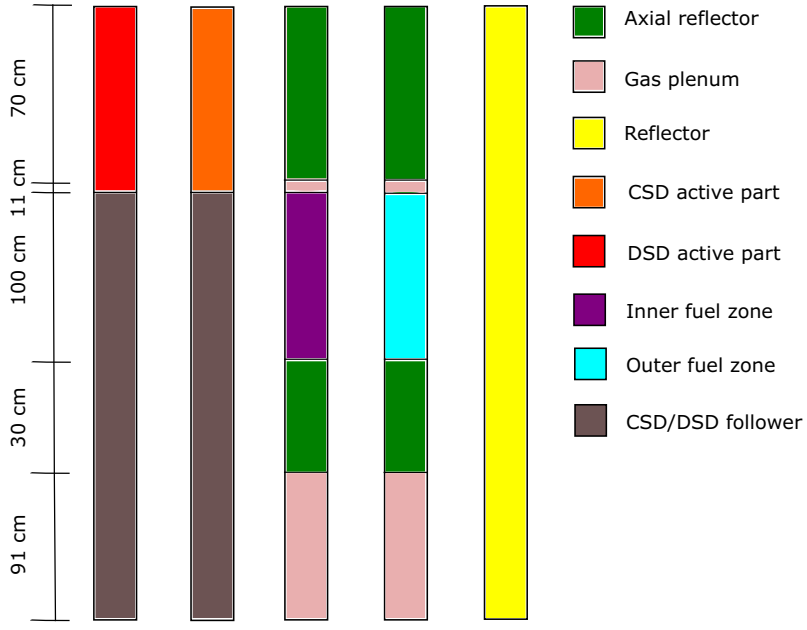

Fig. 3. Axial scheme of the ESFR core.

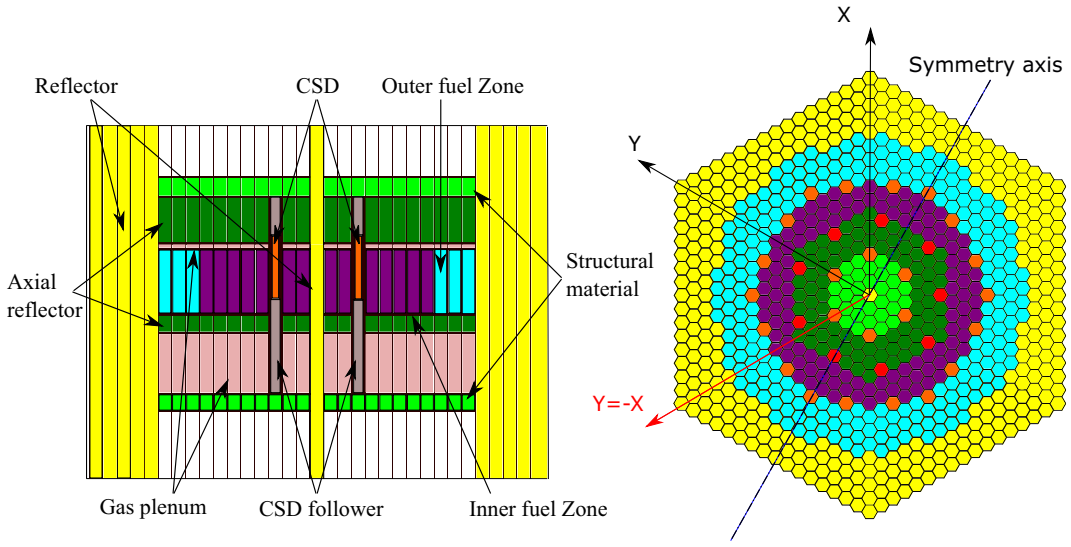

Fig. 4. Axial and radial view of the MCNP6 model of ESFR core. On the right it is shown the radial discretization of the inner fuel zone together with MCNP6 reference coordinate system.

Table 4
Normal operational temperatures of the core components and corresponding cross section library temperatures.

Reactor component	Normal operational temperature (K)	Processed library temperature (K)
Coolant, Gap, Reflector, Structural materials	770	700
Control rod, Control rod followers	970	900
Fuel	1527	1500

positions shown in Table 2 (i.e. from the beginning of life, BoL, condition). Since MCNP6 estimates the new material compositions at the end of each burnup step averaging over the total volume of the material that is burnt, to better follow the fuel depletion as a consequence of the burnup, the inner fuel zone of the reactor core has been divided into three regions filled with the same material but with different identifiers (see Fig. 4). Doing so, three different burned compositions will be produced within the inner fuel zone instead of a single one. Similarly, to have a fuel depletion which can consider the insertion of the control rods up to a certain depth into the core and the axial distribution of the neutron flux, the core has been axially divided into five layers, again, filled with the same material but with different identifiers (see again Fig. 3).

The model has a symmetry axis that allows to study only one half of the reactor. The radial shielding, outside the reflector, is not relevant for the purpose of the present study thus a void boundary condition has been applied to the outer surface of the radial reflector (Fiorini and Vasile, 2011). For what it concerns the nuclear data, the libraries used for this study have been the Joint Evaluated Fission and Fusion File (JEFF), version 3.1.2. This libraries include data for all the relevant isotopes at different temperatures in the range between 293 and 1800 K with an average error of ~2% (Obloinsk et al., 2010). The use of this libraries limits the calculation errors because each material is defined making use of cross section files evaluated at temperatures close to those expected during normal operation. Table 4 shows for each component the difference between the expected normal operational temperature and that at which the cross sections have been processed.

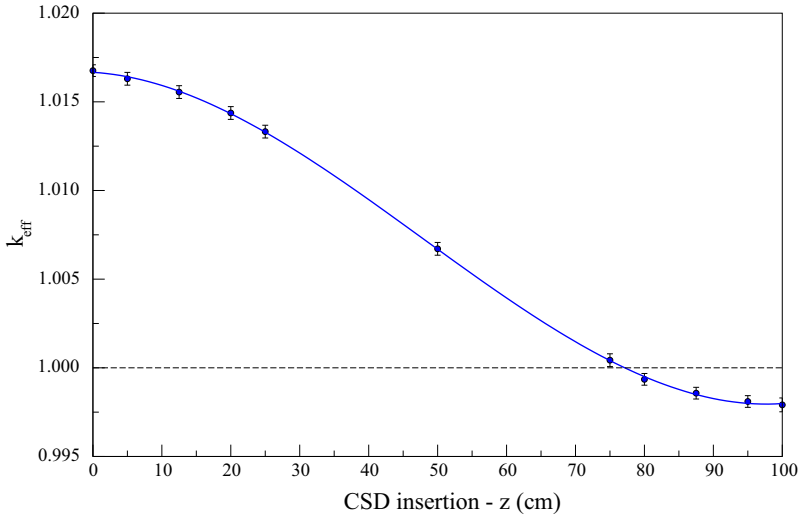

Fig. 5. k_{eff} as a function of the CSD rod insertion (for $z = 0$ the active part of the CSD is completely extracted from the active core region while for $z = 100$ the active part of the CSD is completely inserted inside the active core).

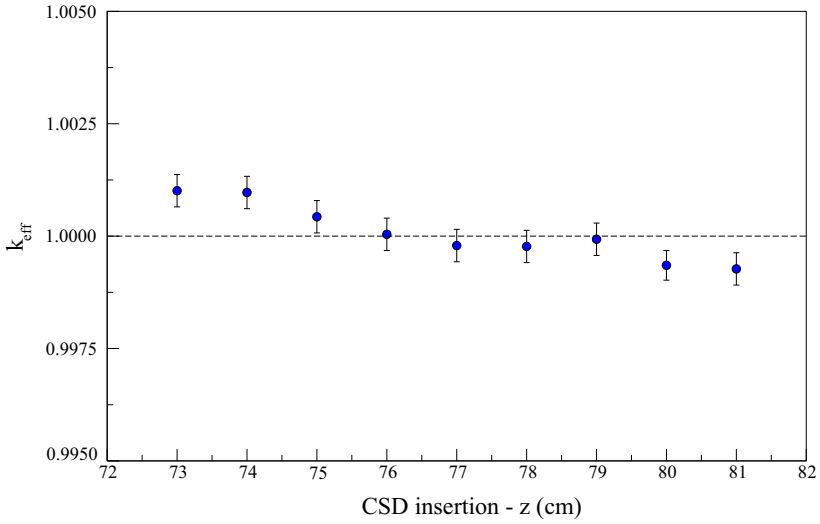

Fig. 6. k_{eff} *versus* CSD rod insertion, detailed calculation across the interval where the reactor is expected to be critical at BoL.

Table 5
k_{eff} evolution during the first burnup cycle. The accuracy of the values is ±0.00031.

Time	k_{eff}
0	0.99998
1	0.99980
2	0.99937
2.5	0.99944
3.5	0.99943
5	0.99892
9.5	0.99892
17	0.99884
32	0.99874
92	0.99858
152	0.99891
212	0.99908
272	0.99907
332	0.99940
365	0.99923

3. Determination of the power peaked fuel assemblies at EoC

3.1. Simulation of the reactor criticality and burnup calculation

In order to achieve the main goal of this work, i.e. the evaluation of the axial and radial fission power distribution inside the power peaked fuel pin at EoC under an unprotected transient of over-power, two preliminary steps were needed. The first step has been the estimate of the CSD rod position returning a critical reactor (i.e. with an effective multiplication constant, k_{eff}, equal to one) at BoL. A set of criticality calculations was then performed moving, all together, the 24 CSD rods inside the reactor core. Each criticality calculations was done using $3 \cdot 10^4$ neutrons per cycle for a total of 500 cycles, the first 50 of which were not considered for the estimate of the effective multiplication constant (inactive cycles). Fig. 5 shows the values of the effective multiplication constant as a function of the insertion of the CSD rods (z coordinate) in the active region of the reactor core ($z = 0$ corresponds to the condition of CSD rods completely withdrawn from the active core region). It

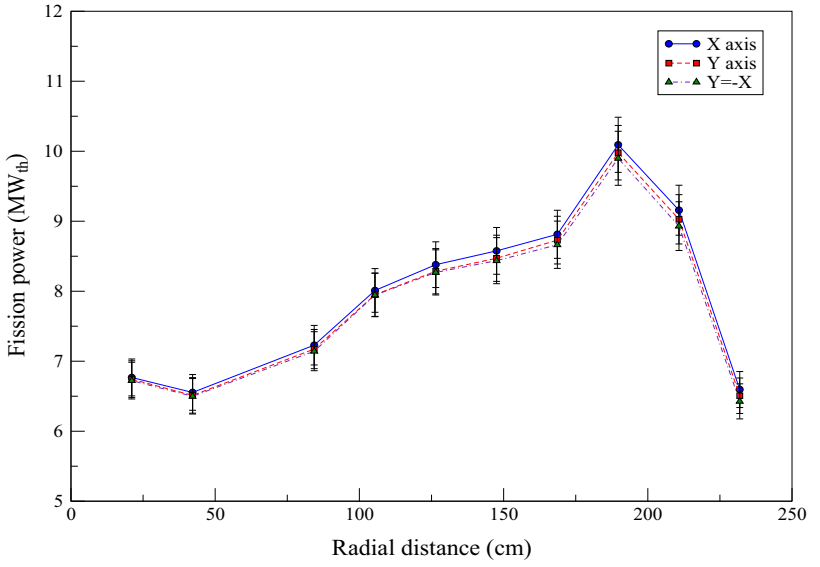

Fig. 7. Fission power along the three considered directions.

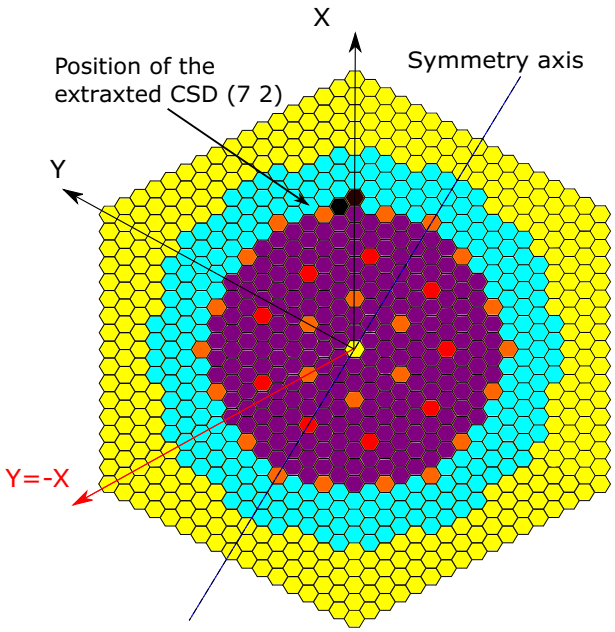

Fig. 8. Fuel assemblies, in black, chosen for the detailed analysis of the fuel pin fission power. The CSD rod removed to simulate the UTOP is also indicated.

can be observed that the curve has the classical sigmoid shape almost symmetric with respect to the middle of the core height ($z = 50$ cm), the different compositions of the top and bottom of the reactor core prevent indeed a full symmetry. Further investigations of the interval between $z = 73$ cm and $z = 81$ cm, see Fig. 6, have shown that the criticality is achieved with the CSD rods inserted at a depth within the interval 76–79 cm. To the midpoint of this interval, 77.5 cm, it corresponds $k_{eff} = 0.99998 \pm 0.00031$ and thus it has been chosen as the position at which the CSD rods have to be set at the BoL.

Under the above critical conditions at BoL, a set of MCNP6 simulations aiming at the estimate of the fuel averaged delayed neutron fraction, β_{eff} was also performed. The use of the *totnu* card in MCNP6 allows the user to consider in the simulation the prompt and delayed or prompt only fission neutrons. Running 500 cycles (the first 50 of which inactive), each one with $3 \cdot 10^5$ starting neutrons, a value of β_{eff} equal to 397 pcm was found. This value is in a good agreement with that shown in Table 1. The number of neutron histories per cycle has been here increased, with respect to the previous criticality calculations, by an order of magnitude to reduce the β_{eff} statistical error down to 6.0%. With the reactor core in the above defined criticality condition at BoL, the second preliminary step has been a burnup/depletion calculation aimed at defining the isotopic composition of the fuel at the end of the first fuel cycle, assuming a cycle length of 365 EFPD (Fiorini and Vasile, 2011). For computational purposes, the fuel cycle was divided into 14 time intervals or burnup steps and the steady-state criticality calculation for each one of them was performed using again 500 cycles (50 inactive) of $3 \cdot 10^4$ neutrons each. Table 5 shows the variation of the k_{eff} during the first fuel cycle, it can be noticed that at the end of the fuel cycle, without moving the CSD rods from their initial position, the reactor core is expected to have a $k_{eff} = 0.99923 \pm 0.00031$, i.e. only 75 pcm lower than that corresponding to the fresh-fuel loaded core, a value which is consistent with previous findings (Thomas, 2015).

3.2. Power peaked fuel assemblies

Once the fuel composition at the end of the first cycle is known it is possible to start searching, among the 122,763 fuel pins within the core, the power peaked one. As the computing time is proportional to the quantity of tallies, the estimate of the fission power of all the fuel pins in a single calculation would result into an excessive computational burden. Thus a first simulation was aimed at finding the region of the core where the power peaked fuel assembly is located, it is, in fact, reasonable to expect that the power peaked fuel pin would be inside this assembly. To investigate the fission power as a function of the distance from the center of the core, according to the MCNP6 internal coordinate system the F7 tally was requested along the axes: $x = 0$, $y = 0$ and $y = -x$ (see Fig. 4 on the right), setting 500 cycles (10% inactive) each one with a number of neutron histories equal to $3 \cdot 10^5$. The tallies results, normalized with respect to the reactor power, indicates that the first ring of fuel assembly in the outer region of the core is where the fuel assembly with the highest power is expected to be located (see Fig. 7).

Hence determined the distance at which we can reasonably expect to have the most power fuel assembly, a new simulation, with the same number of cycles and neutron per cycle, tallying the fission power within 40 fuel assemblies located into this region was performed. The results of this analysis show that the power peaked fuel assembly is that referenced as (90), i.e. the tenth assembly along the positive direction of the x axis, for which the estimated total fission power is equal to 10.1 MW (±0.11%), while the assembly average power of the whole core is equal to 7.9 MW.

4. Results and discussions

The unprotected transient of overpower considered in this study is the consequence of an unexpected runaway of a CSD rod. Since from the previous analysis it has been found that the fuel assembly with the highest fission power is the (90), the CSD rod closer to this assembly, i.e. that in position (72), has been chosen as the ejected one (see Fig. 8). As a consequence of this choice, it has been decided to search for the power peaked fuel pin also within the assembly (81) which is characterized by a fission power of 9.5 MW (±0.11%) and is positioned exactly between the most powered assembly and the ejected control rod.

A MCNP6 simulation with $3 \cdot 10^4$ neutron histories and 500 cycles (10% inactive) was performed in order to estimate the reactivity insertion after the (72) CSD rod ejection. Since the returned value was about 107 pcm, i.e. some 0.27$, it was decided to consider also the simultaneously ejection of two distinct CSD rods, in order to achieve a reactivity insertion closer to the value of β_{eff} and as a consequence a more challenging scenario for the power peaked fuel pin. A second MCNP6 simulation with both the (72) CSD rod and its symmetric with respect to the x axis, the (9 −2) CSD rod, extracted, showed that the reactivity insertion is expected to be of about 270 pcm, i.e. some 0.68$. Finally, it has been decided to consider both the above scenarios in the search of the power peaked fuel pins as the runaway of a single CSD rod represents a design basis accident while the runaway of two CSD rods produces more challenging conditions under which to verify the fuel cladding safety margins.

4.1. Fuel assembly level: search of the power peaked pins

To search for the power peaked pins under the above mentioned conditions, three MCNP6 simulations, with $3 \cdot 10^6$ neutron per cycle and 500 cycles (10% inactive), were then initialized for

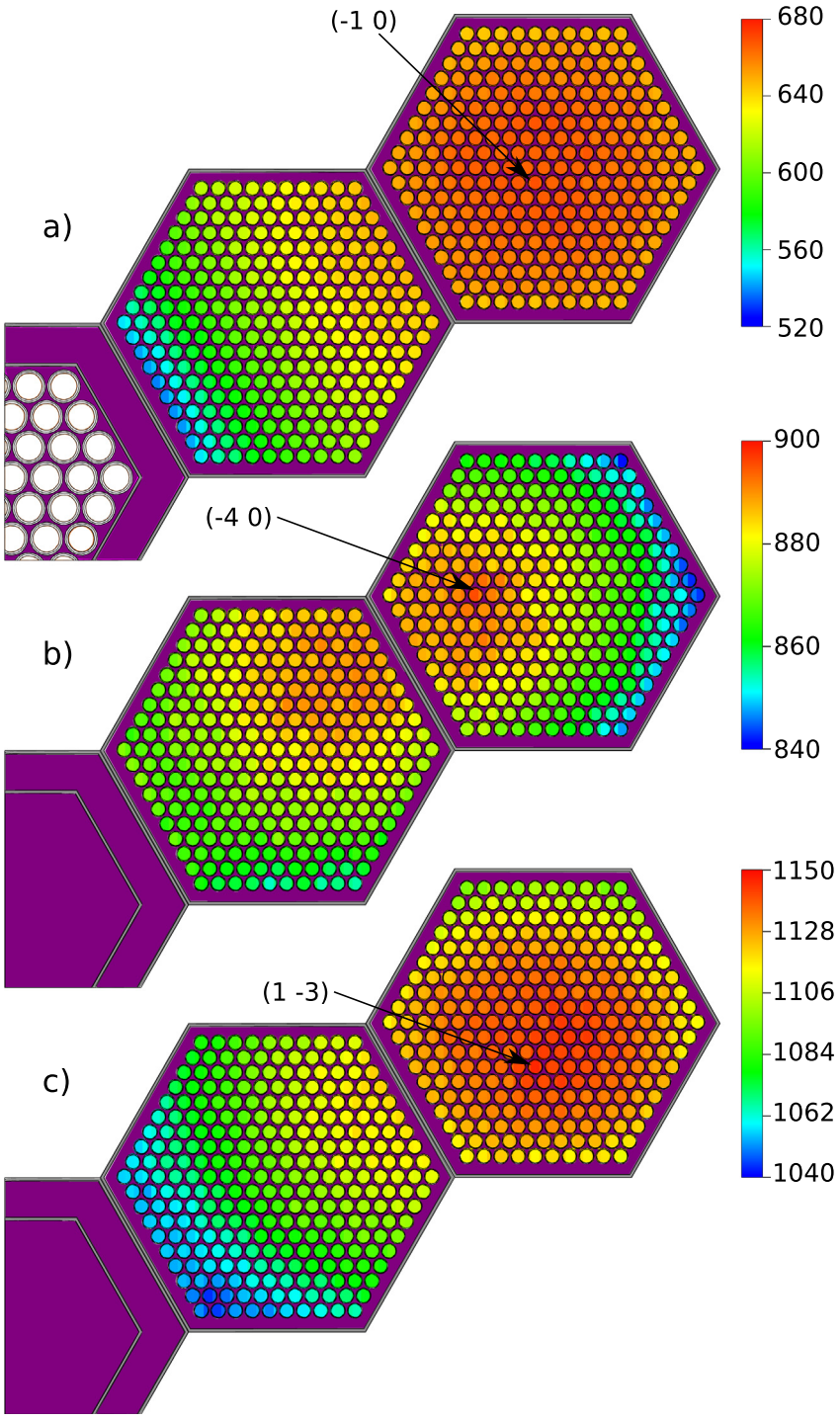

Fig. 9. Distribution of the peak fission power density, in W/cm^3. (a) Normal operation, (b) 1 CSD ejected, (c) 2 CSDs ejected.

the following different scenarios: normal conditions; ejection of the (72) CSD rod; ejection of both the (72) and (9−2) CSD rods. The different results obtained are depicted in Fig. 9 in terms of power density peak. As expected, it can be noted that the power peaked fuel pin changes as the conditions change from the normal operation to the two accidental cases. It appears that under normal operating conditions the region with the highest power density is right in the middle of the fuel assembly (90) and the power peaked fuel pin is the one in the position (−10) which is characterized by a power density of 658 W/cm^3 (see Fig. 9); it is also interesting to note the effect of the CSD rod on the power density in the left side of the fuel assembly (81). When only the (72) CSD rod is extracted the power peaked region is shifted to the left and the power peaked fuel pin becomes that in position (−40) with a value of 894 W/cm^3 (see Fig. 9b); in this case, as a consequence of the CSD ejection, the region of the fuel assembly (81) close to the control rod location has a power density higher than that on the right side of the (90) assembly. Finally, when both the (72) and (9−2) CSDs are extracted, the power density shape returns similar to that of normal operation conditions as the extraction of the CSDs is now symmetric (see Fig. 9c) and the power peaked fuel pin is that in position (1−3) with a value of 1144 W/cm^3.

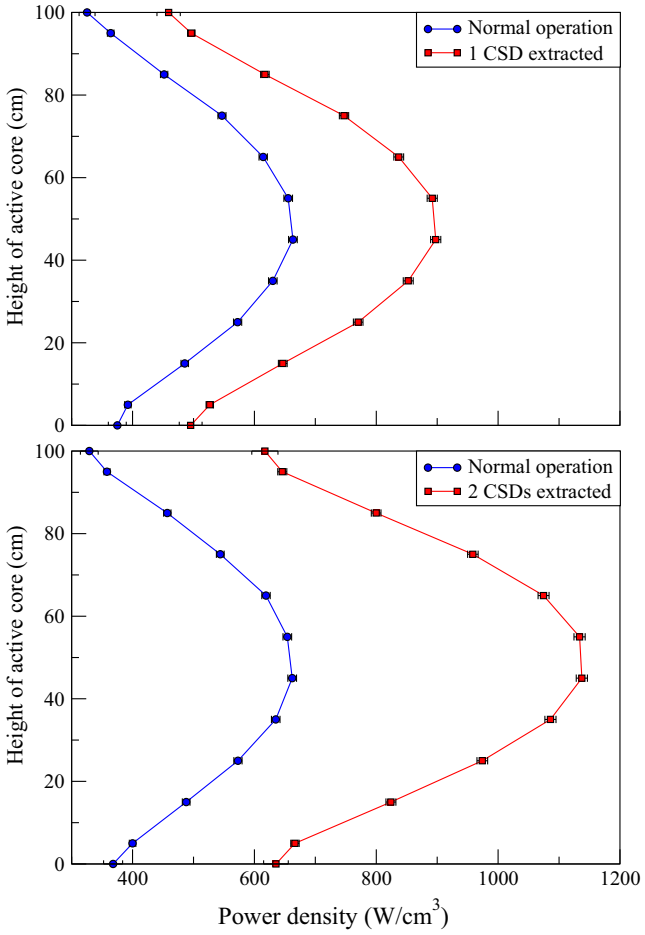

Fig. 10. Axial power density for the power peaked pin in the two accidental scenarios considered.

4.2. Fuel pin level: analysis of the power peaked pin

Once found the power peaked fuel pins under the conditions of the three considered cases, suitable MCNP6 simulations (with $3 \cdot 10^6$ neutron per cycle and 500 cycles, the 10% of which inactive), were performed in order to estimate the fission axial and radial fission power profiles. As shown in Fig. 10, the axial fission power density has the classical cosine profile while the radial power density (see Fig. 11) is flat as it could be expected in case of a fast reactor, like the ESFR. The self-shielding effect in this case is negligible cause to the longer mean free path of the neutrons with respect to that typical for thermal reactors where the self-shielding is instead more pronounced (Todreas and Kazimi, 1990). Finally, it should be mentioned that for the two points at the top and at the bottom of the axial profile the relative error is higher (~1.6%) as the volume associated to them was smaller with respect to the volume associated to the remaining points thus producing a less accurate statistics for the Tally F7 used to estimate the fission power.

5. Conclusions

The main goal of the present study was the determination of the fission power distribution within the power peaked fuel pin under specific accidental conditions. The accident chosen as reference was the Unprotected Transient of Overpower due to the unexpected runaway of a control rod.

Since the tally of the fission power within each fuel pin of the whole reactor core would represent a too hard computational task, at a first time the analysis was limited to the search, under normal operation conditions, of the most powerful assemblies of the core. The assembly in the position (90) was then identified as the most powerful one with a total fission power of 10.1 MW. Together with this, it was chosen to consider also the assembly in position (81) since it has a total power of 9.5 MW and it is in direct contact with the CSD rod, in position (72), that will be ejected to simulate the UTOP accident. Once identified the assemblies within which to perform the search of the power peaked pins, it was found that the ejection of a single control rod is responsible for the insertion of a positive reactivity of 107 pcm (some 0.27$), thus, in order to test more challenging conditions, it was decided to consider also the simultaneous ejection of two control rods (the already identified (72) CSD rod and its symmetric with respect to the x axis) a case for which it was found that a positive insertion of reactivity of 270 pcm (some 0.68$) can be expected. Under normal operating conditions and in case of the two CSD rod ejection the fission power density distribution appears to be quite symmetric with respect to the x axis and the power peaked fuel pins are, respectively, those in position (−10) and (1−3) with a fission power density of 658 and 1144 W/cm^3. When only one CSD rod, the (72), is

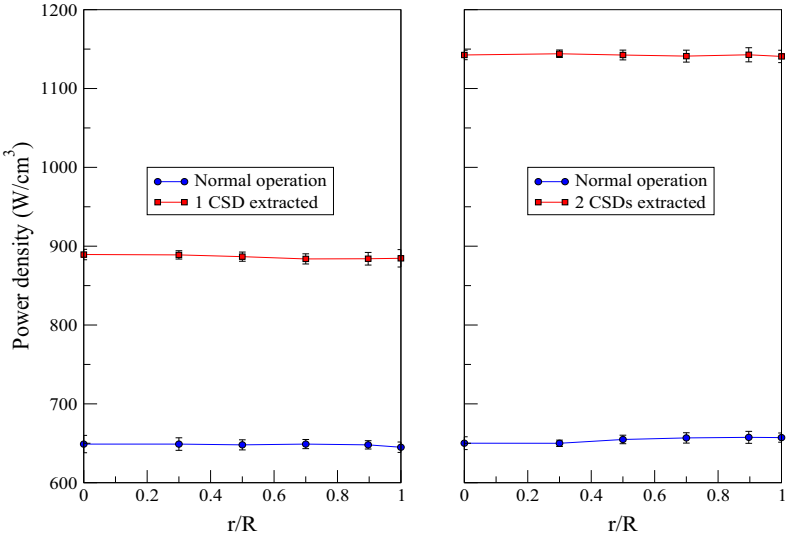

Fig. 11. Radial power density in the central cell (z = 50) of the power peaked pin in the two accidental scenarios considered.

extracted the power peaked region is shifted to the left and the power peaked fuel pin becomes that in position (−40) with a value of 894 W/cm^3. As it concerns the axial and radial distributions of the fission power density within the power peaked fuel pins under the three considered cases, despite the different absolute values which depend on the different conditions, they shows a similar trend: a cosine shape along the fuel axis and a flat distribution along the pin radius. These results are fully consistent with a fast nuclear reactor like the ESFR. In particular the absence of a pin self-shielding is the consequence of the long mean free paths of the neutrons which can then fly over the fuel pin quite easily found for the power peaked fuel pins.

Finally these results will be used as input data for a future assessment of the mechanical safety margin of the pin cladding as well as to study the pellet-cladding mechanical interactions.

Acknowledgements

The authors want to thank Mr. Haileyesus Tsige-Tamirat for sharing the MCNP6 implementation of the ESFR reactor core and for the advices given during the present analysis and Mr. Igor Simonovsky for the help on the cluster installation of MCNP6 and on all the troubles that occurred while the calculation were running.

References

Ammirabile, L., Tsige-Tamirat, H., 2013. Pre-conceptual thermalhydraulics and neutronics studies on sodium-cooled oxide and carbide cores. Ann. Nucl. Energy 60, 127–140.

Chetal, S., Balasubramaniyan, V., Chellapandi, P., Mohanakrishnan, P., Puthiyavinayagam, P., Pillai, C., Raghupathy, S., Shanmugham, T., Pillai, C.S., 2006. The design of the Prototype Fast Breeder Reactor. Nucl. Eng. Des. 236, 852–860 (India's Reactors: Past, Present, Future).

Fiorini, G., Vasile, A., 2011. European Commission 7th framework programme: the collaborative project on European Sodium Fast Reactor (CP ESFR). Nucl. Eng. Des. 241, 3461–3469 (Seventh European Commission conference on Euratom research and training in reactor systems (Fission Safety 2009)).

Goorley, T., James, M., Booth, T., Brown, F., Bull, J., Cox, L.J., Durkee, J., Fensin, J.E., Forster, M., Hendricks, R.A., Hughes, J., Johns, H.G., Kiedrowski, R., Martz, B., Mashnik, R., McKinney, S., Pelowitz, G., Prael, D., Sweezy, R., Waters, J., Wilcox, L., Zukaitis, T., 2012. Initial MCNP6 release overview. Nucl. Technol. 180, 298–315.

Kelly, J.E., 2014. Generation IV International Forum: a decade of progress through international cooperation. Prog. Nucl. Energy 77, 240–246.

Lazaro, A., Schikorr, M., Mikityuk, K., Ammirabile, L., Bandini, G., Darmet, G., Schmitt, D., Dufour, P., Tosello, A., Gallego, E., Jimenez, G., Bubelis, E., Ponomarev, A., Kruessmann, R., Struwe, D., Stempniewicz, M., 2014. Code assessment and modelling for Design Basis Accident analysis of the European Sodium Fast Reactor design. Part II: Optimised core and representative transients analysis. Nucl. Eng. Des. 277, 265–276.

Mi, X., 1999. Chinese fast reactor technology development. In: KAERI-CRIEPI Technical Meeting on LMR. China Institute of Atomic Energy, P. O. Box 275, Beijing 102413, China.

Obloinsk, P., MacFarlane, R., Kahler, A., 2010. Nuclear reaction data methods for processing ENDF/B-VII with NJOY. Nucl. Data Sheets 111, 2739–2890.

Saraev, O.M., Noskov, Y.V., Zverev, D.L., Vasil'ev, B.A., Sedakov, V.Y., Poplavskii, V.M., Tsibulya, A.M., Ershov, V.N., Znamenskii, S.G., 2010. BN-800 design validation and construction status. Atom. Energy 108, 248–253.

Thomas, D.P., 2015. Neutronic analysis of European sodium-cooled fast reactor using Monte Carlo. In: 5th International Youth Conference on Energy (IYCE) 2015 - Pisa, pp. 1–8.

Todreas, N., Kazimi, M., 1990. Nuclear Systems: Thermal Hydraulic Fundamentals. Nuclear Systems. Hemisphere Pub. Corp.

Wilson, W., England, T., George, D., Muir, D., Young, P., 1995. Recent development of the CINDER'90 transmutation code and data library for actinide transmutation studies. In: OSTI (Ed.), Conference: Global '95, Versailles (France), 11 Sep 1995; Other Information: PBD: [1995]. Los Alamos National Laboratories, Los Alamos, NM, USA.